

Consistent spatial scaling of high-severity wildfire can inform expected future patterns of burn severity

Michele S. Buonanduci^{1,2}  | Daniel C. Donato^{2,3}  | Joshua S. Halofsky^{2,3} 
Maureen C. Kennedy⁴  | Brian J. Harvey^{1,2} 

¹Quantitative Ecology and Resource Management, University of Washington, Seattle, Washington, USA

²School of Environmental and Forest Sciences, University of Washington, Seattle, Washington, USA

³Washington State Department of Natural Resources, Olympia, Washington, USA

⁴School of Interdisciplinary Arts and Sciences, University of Washington (Tacoma), Tacoma, Washington, USA

Correspondence

Michele S. Buonanduci, Quantitative Ecology and Resource Management, University of Washington, Seattle, WA, USA.

Email: mbuon@uw.edu

Funding information

Joint Fire Science Program, Grant/Award Number: 21-1-01-26; USGS Northwest Climate Adaptation Science Center, Grant/Award Number: G17AC000218

Abstract

Increasing wildfire activity in forests worldwide has driven urgency in understanding current and future fire regimes. Spatial patterns of area burned at high severity strongly shape forest resilience and constitute a key dimension of fire regimes, yet remain difficult to predict. To characterize the range of burn severity patterns expected within contemporary fire regimes, we quantified scaling relationships relating fire size to patterns of burn severity. Using 1615 fires occurring across the Northwest United States between 1985 and 2020, we evaluated scaling relationships within fire regimes and tested whether relationships vary across space and time. Patterns of high-severity fire demonstrate consistent scaling behaviour; as fire size increases, high-severity patches consistently increase in size and homogeneity. Scaling relationships did not differ substantially across space or time at the scales considered here, suggesting that as fire-size distributions potentially shift, stationarity in patch-size scaling can be used to infer future patterns of burn severity.

KEY WORDS

climate change, fire ecology, high-severity burn patches, scaling relationships, stationarity

INTRODUCTION

Total area burned and the frequency of large fires have increased over recent decades in many forested ecosystems across the globe (Collins et al., 2021; Parks & Abatzoglou, 2020; Whitman et al., 2022). Fire activity is strongly driven by climate (Abatzoglou et al., 2018), and continued increases are expected as fire seasons lengthen, ignitions increase and extreme fire weather occurs more frequently (Bowman et al., 2020). Changing fire activity is expected to further increase area burned and change fire size distributions (Boulanger et al., 2018; Littell et al., 2018; Wang et al., 2022), with important implications for the spatial patterns and ecological effects of fire (Collins et al., 2021; Parks & Abatzoglou, 2020), as well as forest resilience (Johnstone et al., 2016) and associated ecosystem services (Lecina-Diaz et al., 2021).

A key characteristic of forest fires is the amount and spatial configuration of area burned at high severity (i.e. areas where most or all trees are killed by fire). The size and spatial structure of high-severity patches directly

shape postfire seed availability and dispersal (Gill et al., 2022), formation and persistence of complex early-seral habitat (Steel et al., 2022), rates of forest regeneration (Harvey et al., 2016b) and carbon uptake (Turner et al., 2004), and likelihood of conversion to nonforest ecosystems (Coop et al., 2020). Within and among individual fire events, spatial patterns of burn severity are shaped by a complex mixture of broadscale drivers (e.g. climate, fire weather) and local-scale constraints (e.g. topography, fuels) (Harvey et al., 2016a; Parks, Holsinger, Panunto, et al., 2018). Within fire regimes (i.e. areas characterized by a prevailing frequency, seasonality and severity of fire activity; Moritz et al., 2011), the relative influence of broadscale drivers and local-scale constraints shapes the typical or expected spatial dimensions of burn severity.

As fire activity increases in many regions worldwide, a critical gap remains in our ability to anticipate burn severity patch size and structure, and therefore potential ecological effects. Nonstationarity is expected in many direct relationships between climatic drivers and

fire activity due to interacting effects of fuel structure and abundance, and this nonstationarity is often seen as a barrier to predicting future fire effects (Newman et al., 2019). In recent decades, total high-severity burned area has increased in many regions, driven by increases in total area burned and the occurrence of large fires (Collins et al., 2021; Parks & Abatzoglou, 2020). However, whether fires are becoming proportionally more severe or homogenous over time, and what should be expected in the future for such trends, remains unclear. High-severity proportion has increased in some regions (Harvey et al., 2016a; Miller et al., 2009; Parks & Abatzoglou, 2020; Singleton et al., 2019) but not others (Collins et al., 2021; Miller et al., 2012; Reilly et al., 2017; Rivera-Huerta et al., 2016; Whitman et al., 2022). In some cases, high-severity burned areas are becoming characterized by larger and/or simpler shaped patches (Reilly et al., 2017; Rivera-Huerta et al., 2016; Stevens et al., 2017), though whether such trends are directly a result of fire size (Harvey et al., 2016a) and are therefore likely to continue in the future is not well tested. Understanding these relationships is key to forecasting burn severity patterns as fire activity increases.

Scaling relationships can provide fundamental insights into how complex system behaviour emerges as a function of event size and have been used to understand various dimensions of fire activity (McKenzie & Kennedy, 2011). Quantifying scaling relationships describing how high-severity patch size and structure change with fire size could offer a means of forecasting the potential range of future fire effects, given projections for increasing area burned and shifting fire-size distributions. High-severity patch size and structure are strongly related to fire size and high-severity proportion (Cansler & McKenzie, 2014; Collins et al., 2017; Harvey et al., 2016a), exhibiting characteristic scaling relationships both within fire events and within fire regimes. Across fire size distributions, scaling behaviour arises in theory because the potential for large high-severity patches scales upward with the size of fire events (Gardner & Urban, 2007). In reality, the relative influence of broadscale drivers versus local-scale constraints will dictate, to varying degrees, the occurrence of increasingly large and contiguous high-severity patches with increasing fire size (Cansler & McKenzie, 2014; Harvey et al., 2016a). Therefore, the forms of these scaling relationships are expected to vary by fire regime, and as with other facets of fire activity, to operate within some characteristic range of variation (Moritz et al., 2011). By integrating system-level interactions between climate and fuels, scaling relationships have the potential to exhibit stationarity and thus offer a credible approach to projecting future fire effects. Despite the potential for scaling relationships to yield insight into the ranges of burn severity patterns that emerge within fire regimes, these relationships have not yet been widely explored.

Here, we address the above knowledge gap by asking what spatial patterns of burn severity, and therefore ecological effects, are expected from fires of different sizes. Using contemporary (1985–2020) satellite burn severity data, we quantify spatial scaling relationships using 1615 fires occurring across a gradient of fire regimes (frequent and low severity, moderately frequent and mixed severity, and infrequent and high severity) within a $>600,000 \text{ km}^2$ forested region (the Northwest United States; Figure 1), asking: (Q1) *What is the contemporary range of variation in high-severity patch size and structure expected from fires of different sizes?* (Q2) *Do spatial scaling relationships vary by geographic region and/or time period (i.e. do they appear stationary in space and/or time)?* To address these questions, we fit smooth curves to multiple conditional quantiles of each metric across the range of observed fire sizes (400 – $>400,000 \text{ ha}$). We thereby evaluate how the upper and lower bounds of high-severity patch size and structure (in addition to central tendency estimates) scale with fire size. To evaluate spatial and temporal stationarity, we test whether the scaling relationships that characterize fire regimes vary by geographic region (Pacific Northwest versus Northern Rockies; Figure 1), year, or time period [1985–2000 versus 2001–2020, the latter period being associated with increasing aridity and accelerating annual area burned in the western United States (Juang et al., 2022)]. As fire size distributions shift in the future, stationarity in the relationships between fire size and patterns of burn severity would enable future broadscale patterns of burn severity to be inferred.

MATERIALS AND METHODS

Study region

Our study region is the forested ecoregions of the Northwest United States (Wyoming, Montana, Idaho, Washington, Oregon, and northern California), delineated using EPA Level III Ecoregions (Commission for Environmental Cooperation, 1997) (Figure 1). Climate, topography and forest types vary widely across the study region, as do fire activity and fire-adapted traits of dominant tree species (Hood et al., 2021; Reilly et al., 2021; Stevens et al., 2020). Historical fire regimes range from frequent, low-severity fire in warmer and drier parts of the region to infrequent, high-severity fire in cooler and wetter parts of the region (Hood et al., 2021; Reilly et al., 2021). We used LANDFIRE land cover data to classify forested areas and fire regime groups (FRGs) throughout the study region (Rollins, 2009). We identified potentially forested areas using LANDFIRE Environmental Site Potential (ESP) and classified the study region into three historical fire regimes: frequent and low severity (FRG I), moderately

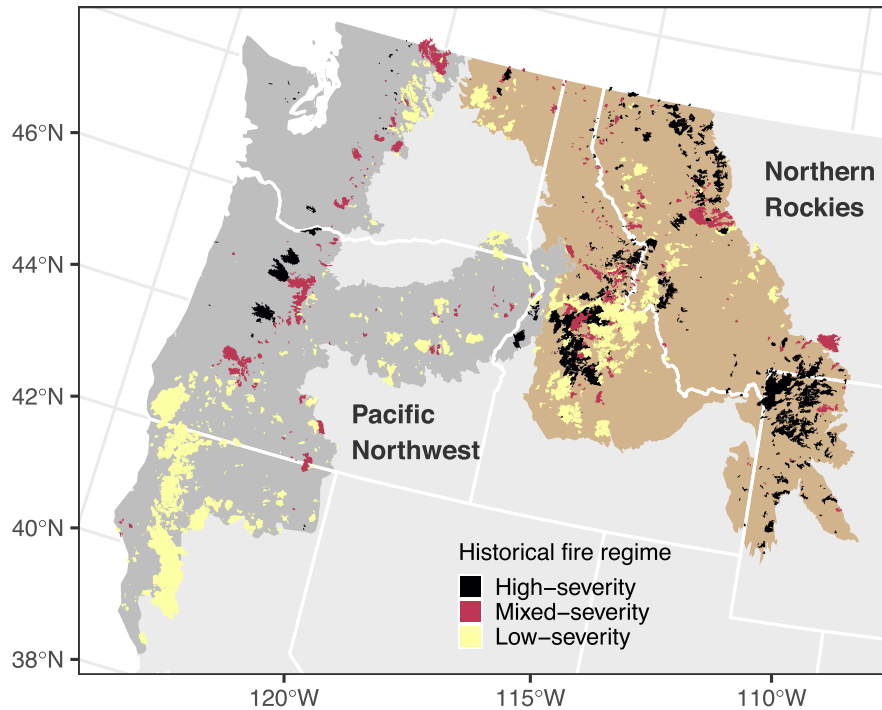


FIGURE 1 Study region with all wildfires categorized by primary historical fire regime (frequent and low-severity, moderately frequent, and mixed-severity, infrequent and high-severity). Fire regime classifications are from the LANDFIRE database (Rollins, 2009).

frequent and mixed severity (FRG III), and infrequent and high severity (FRG IV and FRG V).

Fire severity data

We obtained perimeters for all fire events ≥ 400 ha in size occurring within the study region between 1985 and 2020 from the Monitoring Trends in Burn Severity database (<https://mtbs.gov/>). We included only those fire events occurring in primarily forested areas ($\geq 50\%$ forested based on LANDFIRE ESP) that were designated wildfires (i.e. we excluded prescribed fires). Each fire event was assigned its dominant historical fire regime (low-, mixed- or high-severity) based on the most prevalent fire regime group within that fire's perimeter (Figure 1). In total, our data set consisted of 1615 individual fire events, with 751, 373, and 491 fire events assigned to the low-, mixed- and high-severity fire regime groups, respectively.

Burn severity maps were generated for each fire event using Landsat satellite data and following previously established methods (Parks, Holsinger, Voss, et al., 2018). We quantified burn severity at a 30-m pixel scale using the relativized differenced normalized burn ratio (RdNBR), a satellite-based fire severity metric that estimates the amount of fire-induced vegetation change by comparing pre- and postfire vegetation greenness indices (Miller & Thode, 2007). We included an offset term in our calculation of RdNBR to account for phenological differences between pre- and postfire imagery (Parks, Holsinger, Voss, et al., 2018). Following Harvey et al. (2023), we

used statistical models calibrated to Northwest United States field plots (Saberi & Harvey, 2023) to identify a threshold of RdNBR ($RdNBR \geq 542$) corresponding to $\geq 75\%$ tree basal area mortality. We then used this threshold to categorize each burn severity map into high ($RdNBR \geq 542$) and low-to-moderate ($RdNBR < 542$) burn severity classes. High-severity classifications based on satellite index thresholds regularly have the highest accuracy relative to other burn severity classes (Cansler & McKenzie, 2012; Lydersen et al., 2016; Miller & Thode, 2007), and similar thresholds for high-severity fire have been applied across a range of scales, from regional extents (Reilly et al., 2017; Singleton et al., 2019; Stevens et al., 2017) to the entirety of the western United States (Davis et al., 2023; Parks, Holsinger, Panunto, et al., 2018).

Landscape metrics

Our analysis focussed on areas within each fire event that burned at high severity, quantifying landscape metrics describing both the size and spatial configuration of high-severity patches. High-severity patches were delineated using an eight-neighbour rule after a majority smoothing filter was applied to each categorized burn severity map to reduce the impact of single-pixel patches (Figure 2a). Within each high-severity patch, distance to seed source was quantified for each pixel that was potentially forested prior to burning. Distance to seed source was quantified by calculating the distance to the nearest

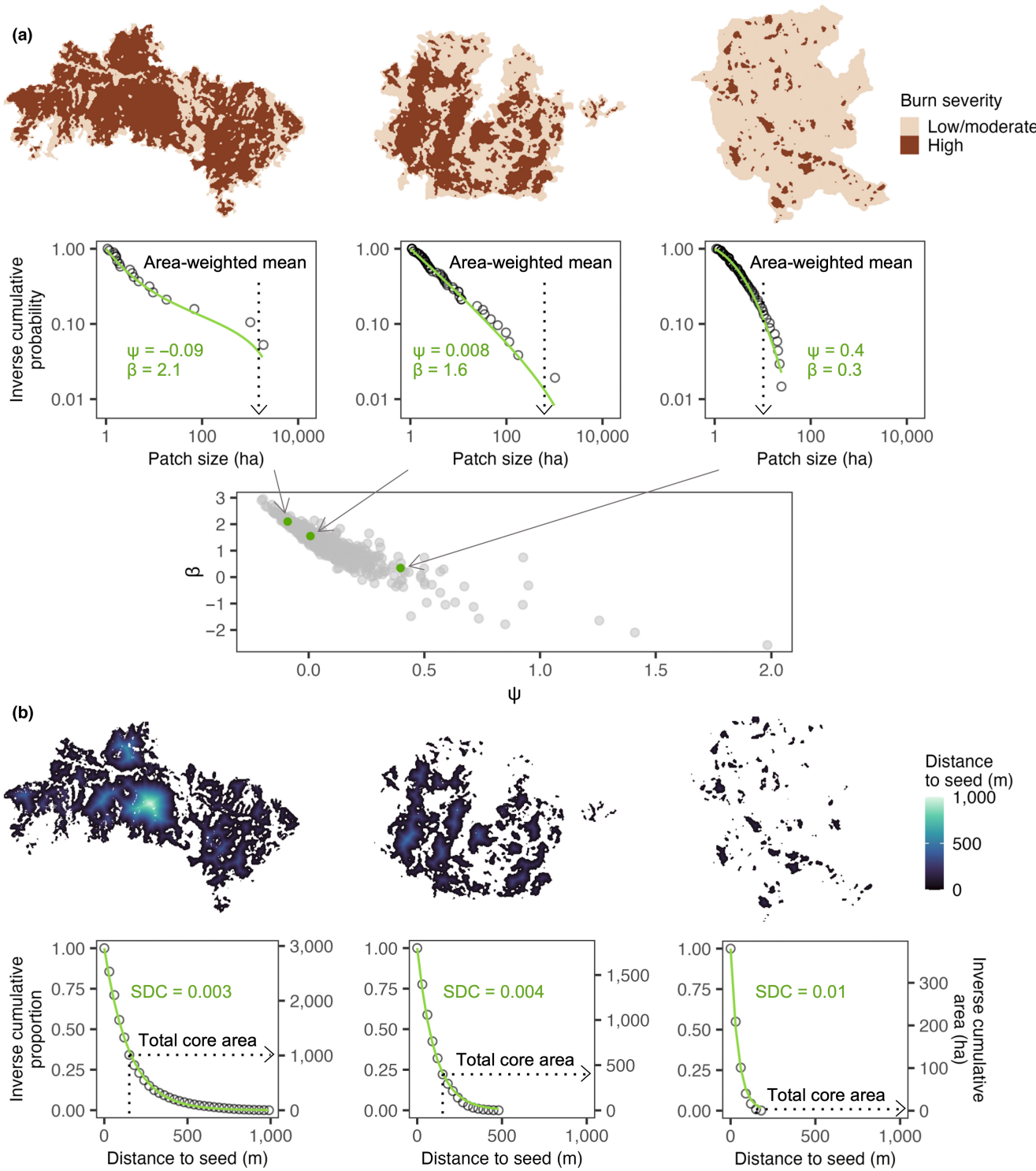


FIGURE 2 Schematic illustrating high-severity patch size (a) and high-severity patch structure (b) metrics for three wildfires that were similar in size (each 4000–4500 ha). Open circles represent observed data within each fire event, black dotted lines with arrows point to standard (aggregate or central tendency) metrics, and solid green lines represent metrics describing within-fire distributions. (a) Patch size metrics include area-weighted mean patch size and two parameters (ψ and β) describing the shape of the patch size distribution. When ψ is close to zero, patch size distributions resemble a power law function. When ψ is negative, patch size distributions curve upward and are typically characterized by one or more very large patches. When ψ is positive, patch size distributions curve downward and are typically characterized by many small patches. Scatter plot of ψ and β shows parameter values for all fires in the dataset. (b) Patch structure metrics account for patch shape and forest cover and include total high-severity core area (previously forested pixels >150 m from potential unburned seed source following fire) and one parameter (SDC) describing the shape of the distance-to-seed distribution for forested areas burned at high severity. Smaller values of SDC represent larger and more homogenously shaped patches with interior areas far from unburned seed sources. From left to right, example fires are the Fishhawk (Wyoming), Boze (Oregon), and Big Bend (Oregon) fires.

potentially forested pixel that did not burn at high severity ([Figure 2b](#)).

We quantified the size of high-severity patches using two complementary approaches ([Figure 2a](#)). First, we calculated the area-weighted mean size of all high-severity patches within each fire event. By weighting larger patches more heavily, an area-weighted mean is larger than an arithmetic mean and represents the expected patch size that would be encountered in an average location within a landscape (Harvey et al., [2016a](#)). Second, we characterized the shape of each patch size distribution using an approach that has, to the best of our knowledge, not previously been used to describe high-severity patch size distributions within fire events. Following the methods developed for fire size distributions by Hantson et al. ([2016](#)), we fit truncated lognormal distributions to the patch sizes within each fire event. The probability density function, $p(x)$, for each patch size distribution takes the following form:

$$\ln p(x) = \ln C - \beta \ln(x) - \psi[\ln(x)]^2$$

where C is a normalization constant, ensuring the area under $p(x)$ sums to 1, and takes the following form:

$$C = \left(\int_{x_{\min}}^{x_{\max}} e^{-\beta \ln(x) - \psi[\ln(x)]^2} dx \right)^{-1}$$

The parameters x_{\min} and x_{\max} define the lower and upper truncation limits, respectively. We set x_{\min} equal to 1 ha and x_{\max} equal to the size of each individual fire event. Essentially, $p(x)$ is a modified truncated power law function with an added term, ψ , that adds curvature to the distribution in log–log space (Pueyo, [2006](#)). Within the truncation limits, the parameters β and ψ determine the shape of each distribution ([Figure 2a](#)). When ψ is equal to 0, the distribution reduces to a power law function, and the shape of the distribution is a straight line in log–log space, with β determining the slope, or relative prevalence of small versus large patch sizes. When ψ is negative, the distribution curves upward in log–log space (i.e. there is a greater likelihood of large patches, relative to a power law function with the same value of β). When ψ is positive, the distribution curves downward in log–log space (i.e. there is a lower likelihood of large patches, relative to a power law function with the same value of β). In practice, the parameters β and ψ are highly correlated, with β decreasing as ψ increases ([Figure 2a](#)) (Hantson et al., [2016](#)).

As with the size of high-severity patches, we quantified the spatial structure of high-severity patches using two complementary approaches ([Figure 2b](#)). First, we calculated total core area within the interior of high-severity patches, where core area is defined as previously forested pixels >150 m from potential seed source following fire. This threshold of 150 m exceeds the likely seed dispersal

distance for many conifers in the Northwest United States (Donato et al., [2009](#); Harvey et al., [2016b](#)). Second, using the approach proposed by Collins et al. ([2017](#)), we characterized the rate at which the forested area within the interior of high-severity patches shrinks with increasing distance to potential seed source. In this approach, the proportion of total high-severity or ‘stand-replacing’ forested area, P , exceeding a given distance to potential seed, dts , is modelled using a modified logistic function as follows:

$$P \sim \frac{1}{10^{SDC \times dts}}$$

Here, the stand-replacing decay coefficient (SDC) is a parameter determining the rate at which the proportional stand-replacing area decreases with increasing distance to potential seed. Larger values of SDC indicate a rapidly decaying interior area (i.e. most forested areas burned at high severity are relatively close to potential seed sources), whereas smaller values of SDC indicate a more slowly decaying interior area (i.e. more forested areas burned at high severity are far from potential seed sources; Collins et al., [2017](#)).

Area-weighted mean patch size and total core area were calculated using the *sf* and *raster* packages in R (Hijmans et al., [2022](#); Pebesma, [2018](#)). Patch size distribution shape parameters (β and ψ) were fit to the patch size distributions for each fire event using the maximum likelihood algorithm proposed by Pueyo ([2014](#)). We only fit patch size distribution parameters for fire events with at least 10 patches that were ≥ 1 ha in size ([Table S1](#)). Distance-to-seed distribution parameters (SDC) were fit to the inverse cumulative distance-to-seed distributions for each fire event using nonlinear least squares, following Collins et al. ([2017](#)). Inverse cumulative distance-to-seed distributions were summarized using 30-m bins of pixel-level distance to potential seed source prior to parameter fitting, and parameters were fit only to those fire events with high-severity area falling within at least two 30-m bins ([Table S2](#)).

Analysis

We used nonparametric quantile regression to quantify the range of variation in high-severity patch size and structure metrics expected from fires of different sizes ([Q1](#)). Compared with standard regression approaches, which estimate the conditional mean of a response variable, quantile regression estimates the conditional quantiles of a response variable, thereby providing a fuller picture of the relationships between variables (Cade & Noon, [2003](#); Koenker & Bassett, [1978](#)). This approach is particularly useful in ecological applications where complex interactions between multiple variables, many of which cannot be accounted for, lead to unequal variances

in response distributions (Cade & Noon, 2003). Rather than assuming linearity in scaling relationships, we used a nonparametric approach to fit smooth curves (via additive basis splines) to the conditional quantiles of each scaling relationship (Muggeo et al., 2021).

We fit smooth curves to five conditional quantiles (0.05, 0.25, 0.5, 0.75, and 0.95) of each patch size and structure metric across the range of observed fire sizes within each fire regime. Quantile curves were constrained to be monotonically increasing for area-weighted mean patch size and total core area, both of which are expected to continually increase with fire size (Cansler & McKenzie, 2014; Harvey et al., 2016a; Reilly et al., 2017), and monotonically decreasing for the distance-to-seed parameter (SDC), which is expected to continually decrease with fire size (Collins et al., 2017). No monotonicity constraints were imposed for the patch size distribution parameters (β and ψ). Area-weighted mean patch size, total core area, and SDC were \log_{10} -transformed prior to model fitting; in cases where total core area was zero, we added 0.01 ha to enable \log_{10} -transformation. To evaluate potential differences between fire regimes, we also fit combined models for each metric with smooth terms for fire size that were allowed to vary by fire regime. We then evaluated whether there were significant differences between fire regime-specific scaling relationships by calculating pointwise differences, along with approximate 95% confidence intervals, between pairs of regime-specific quantile curves across the range of observed fire sizes following Rose et al. (2012). All quantile curves were fit using the *quantregGrowth* package in R (Muggeo, 2021).

We used multiple lines of evidence to evaluate the spatial and temporal stationarity of scaling relationships (Q2). To evaluate spatial stationarity, we considered two broad geographic regions within our study area: the Pacific Northwest and the Northern Rockies (Figure 1). Unfortunately, within the high-severity fire regime, there were too few fire events in the Pacific Northwest ($n=42$) for a robust comparison with the Northern Rockies ($n=449$) (Tables S1, S2). Within the low- and mixed-severity fire regimes, however, we fit quantile regression models with smooth terms for fire size that were allowed to vary by geographic region. We then evaluated whether there were significant differences between region-specific scaling relationships by calculating pointwise differences between region-specific quantile curves, along with approximate 95% confidence intervals, following the approach used for fire regimes.

To evaluate temporal stationarity, we considered annual trends and two distinct time periods: an early period (1985–2000) and a late period (2001–2020), the latter of which is associated with increasing aridity and accelerating annual area burned in the western United States (Juang et al., 2022). Within each fire regime, we fit three sets of quantile regression models. First, to assess interannual variation, we fit models with smooth terms for

fire size and additional smooth terms for year. Second, to test for overall increasing or decreasing trends, we fit models with smooth terms for fire size and additional linear terms for year. Annual trends were considered statistically significant if $p<0.05$ for the linear year term. Third, to evaluate whether there were significant differences between time period-specific scaling relationships, we fit quantile regression models with smooth terms for fire size that were allowed to vary by time period, following the approach used for fire regimes and geographic regions.

As an additional line of evidence, we used a 10-fold cross-validation procedure to evaluate whether adding a smooth term for year or allowing scaling relationships to vary either by time period or geographic region improved model predictive power over a null model (i.e. a model including fire size as the only predictor). Prediction error was calculated for quantiles 0.05, 0.5 and 0.95 using the quantile loss function (Koenker & Bassett, 1978), which asymmetrically weights the absolute residuals and is analogous to the root mean square error used in standard regression models. Prediction error was averaged across quantiles and cross-validation folds for each model, with a reduction in overall average prediction error considered an improvement in model predictive power.

RESULTS

Scaling relationships

Across fire regimes, we observed qualitatively similar scaling relationships for high-severity patch size and structure (Figure 3a–j). Area-weighted mean patch size and total core area consistently increased with fire size (Figure 3a,b,g,h), reflecting the occurrence of increasingly large and spatially homogenous high-severity patches with increasing fire size. The distance-to-seed distribution parameter (SDC) consistently decreased with fire size (Figure 3i,j), indicating greater distances to unburned seed sources within patch interiors. Patch size distribution parameters were highly variable at small fire sizes, but as fire sizes increased, ψ approached a value of 0 and β a value of 1.5 (Figures 2a, 3c–f). This suggests a convergence of patch size distributions toward a power law with increasing fire size.

Spatial scaling relationships were characterized by large ranges of variation, with the low- and mixed-severity fire regimes exhibiting wider ranges of variation for most metrics compared with the high-severity fire regime (Figure 3a–j). Across the range of fire sizes, the upper bounds for potential patch size and homogeneity (i.e. upper quantile estimates for area-weighted mean patch size and total core area, and lower quantile estimates for SDC) did not differ across fire regimes (Figure 3b,h,j, Figure S1). However, the lower bounds for potential patch size and homogeneity (i.e. lower quantile

Patch size metrics

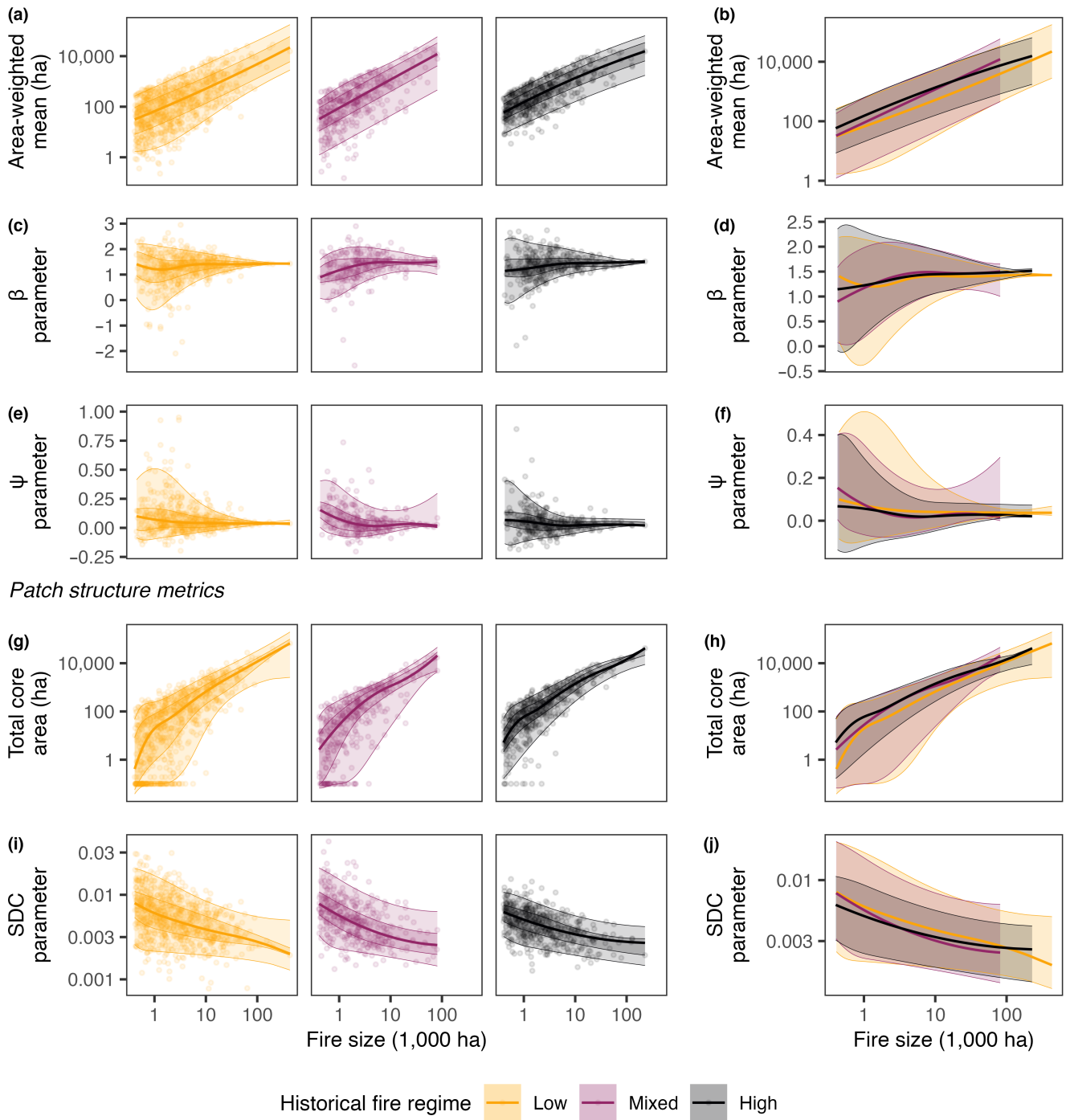


FIGURE 3 Quantile regression estimates for all high-severity patch size (a–f) and high-severity patch structure (g–j) metrics, plotted separately for each fire regime with observed data (left column) and overlaid for comparison across regimes (right column). Dots represent observed data, thick solid line is quantile 0.5, dark shaded region is interval between quantiles 0.25 and 0.75 (shown only in plots with observed data), and light shaded region is interval between quantiles 0.05 and 0.95. Three data points (for which $\psi > 1$) were excluded from (e) to improve visualization of quantile estimates.

estimates for area-weighted mean patch size and total core area, and upper quantile estimates for SDC) varied across fire regimes (Figure 3b,h,j, Figure S1), with smaller and more heterogeneous patches tending to occur in the low- and mixed-severity regimes across the range of fire sizes.

Spatial and temporal stationarity

Within fire regimes, we observed both spatial and temporal stationarity in scaling relationships, as suggested by a lack of strong evidence that scaling relationships differ by region, time period or year. After accounting

for fire regime, region-specific scaling relationships (Pacific Northwest versus Northern Rockies; [Figure 1](#)) largely did not differ (in the low- and mixed-severity regimes, for which data were sufficient for robust regional comparisons; [Figure S2](#)), suggesting that fire regimes are characterized by consistent scaling relationships across space. We observed modest interannual variation in some scaling relationships ([Figure 4](#)); however, in most cases, we detected no linear trend in scaling relationships over time ([Figure 4](#)) or difference in scaling relationships

between time periods [early (1985–2000) versus late (2001–2020)] ([Figure S3](#)), suggesting the relationships between fire size and spatial patterns of burn severity are not yet changing over time and with warming climate. Cross-validation indicated that null models (i.e. models including fire size as the only predictor) offered the highest predictive power in most cases ([Tables S3 and S4](#)); in cases where region, year, or time period did improve model performance, the improvement was slight (prediction error reduced by $\leq 1\%$ compared to null models).

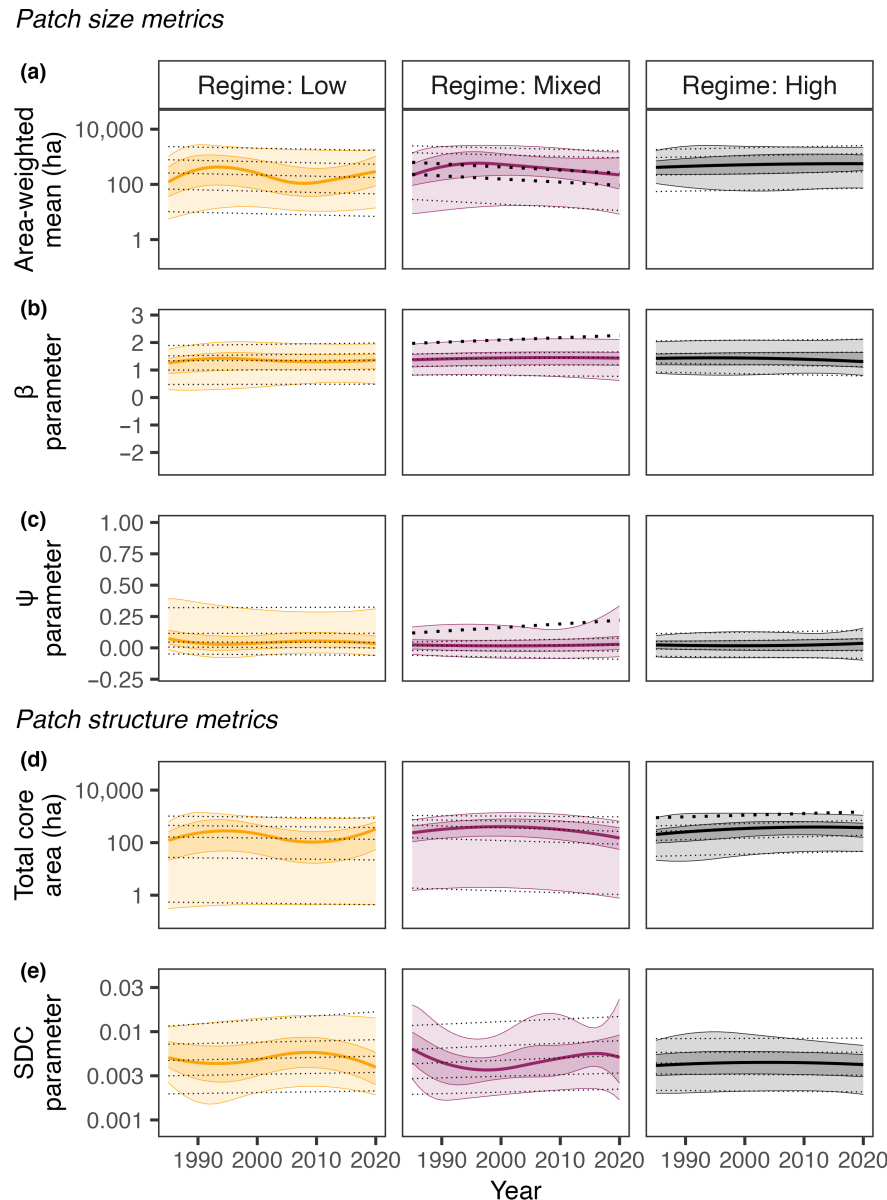


FIGURE 4 Estimated marginal effect of year for all high-severity patch size (a–c) and high-severity patch structure (d,e) metrics. Fire size is held constant at 3000 ha. Solid lines and shaded intervals are quantile estimates from models with smooth term for year; solid line is quantile 0.5, dark shaded region is interval between quantiles 0.25 and 0.75, and light shaded region is interval between quantiles 0.05 and 0.95. Dotted lines are quantile estimates from models with linear term for year; heavy dotted lines indicate linear terms for which $p < 0.05$ and light dotted lines indicate linear terms for which $p \geq 0.05$. Linear terms were generally not statistically significant, suggesting temporal stationarity in the relationship between fire size and spatial patterns of burn severity.

DISCUSSION

Our findings demonstrate that spatial patterns of high-severity wildfire scale consistently with fire size, a phenomenon with important implications for how forests are shaped by increasing fire activity now and in the future. The robust scaling relationships that emerged within and among a range of forest ecosystems and fire regimes reveal characteristic signatures of contemporary forest fire activity. These scaling relationships, which appear stationary in both space and time at the scales considered here, offer a powerful means to anticipate near-future patterns of burn severity as climate warming continues and fire sizes increase across ecosystems.

Scaling relationships emerge within and among fire regimes

High-severity patch size and structure followed clear scaling relationships that were qualitatively similar across fire regimes, demonstrating that across contemporary forest systems, larger wildfires consistently result in larger and more homogenous patches of severe fire effects. With greater fire size, high-severity patches tended to be larger and more spatially homogenous (greater area-weighted mean patch size and total core area), containing areas that were increasingly far from potential seed sources (lower SDC). In forested ecosystems that rely on seed dispersal for postfire recovery, larger and simpler shaped high-severity patches can alter forest resilience, as these areas are more likely to regenerate slowly and to transition to nonforest vegetation states following fire (Coop et al., 2020).

Quantifying multiple conditional quantiles of patch size and structure revealed key similarities and differences in the ranges of burn severity patterns across fire regimes. The fire regimes in our study span a gradient of climate- to fuel-limitation, with fire activity in the infrequent, high-severity fire regime being primarily climate-limited and fire activity in the frequent, low-severity fire regime being primarily fuel-limited (Hood et al., 2021; Reilly et al., 2021). In the absence of other limiting factors, fire size itself imposes some natural upper limit to the size and homogeneity of high-severity burn patches. As limitations on fire severity increase in number and/or relative influence (e.g. in landscapes with complex topography, discontinuous fuel structure, and/or moderate fire weather conditions), patches are expected to become smaller in size or more complex in shape (Cansler & McKenzie, 2014; Harvey et al., 2016a), therefore falling below the fire-size-imposed upper limits. Among fire regimes, the comparable upper bounds for patch size and homogeneity across the range of fire sizes suggests that when the influence of local-scale constraints is relatively weak (e.g. under extreme fire weather conditions), fire size itself imposes a comparable

upper limit to patch size and structure across systems. In the low- and mixed-severity regimes, patches tended to fall below these fire-size-imposed upper limits more frequently than in the high-severity regime, with differing lower bounds emerging for patch size and homogeneity among fire regimes. This divergence in scaling relationships across fire regimes reflects the greater influence of local-scale constraints on fire severity in the low- and mixed-severity systems.

Contemporary ranges of variation in scaling relationships likely differ from historical ranges, particularly in the low- and mixed-severity regimes, due in large part to contemporary land management practices. Forests across the Northwest United States have been subject to more than a century of fire exclusion and suppression (Hagmann et al., 2021), which can influence scaling relationships in multiple ways. First, since fire suppression efforts are less successful under extreme weather conditions (Arienti et al., 2006), the largest fires in our data set are more likely to have burned under extreme conditions. In the absence of suppression efforts, a wider range of burn severity patterns for larger fires allowed to burn under mild or moderate weather conditions might be expected. Second, in low- and mixed-severity regimes, fire exclusion has led to an uncharacteristic buildup of fuels and a misalignment of forest structure and fire activity with historical conditions (Hagmann et al., 2021). Prior to European colonization, the low-severity regime was characterized predominantly by frequent but low-severity surface fires (Hood et al., 2021; Reilly et al., 2021). Although we found that burn severity patterns tended to be more heterogeneous in the low-severity regime, we also found that high-severity patches could be as large and homogenous as those observed in the high-severity regime, potentially reflecting this departure from historical conditions. This departure is a major concern for forest resilience in historically low-severity regimes, which are generally not as well adapted to recover from large patches of high-severity fire as are forests within high-severity regimes (Pausas et al., 2017; Stevens et al., 2020).

Patch size distributions within large fires exhibit power law behaviour

The convergence of within-fire patch size distributions toward a power law function with increasing fire size carries implications for the scale of drivers operating within large fires. In the context of regional or global fire size distributions, power law behaviour has been posited to emerge within facets of fire activity when there is a balance between broadscale drivers and local-scale constraints (McKenzie & Kennedy, 2012; Moritz et al., 2011; Povak et al., 2018). Here, the emergence of power law behaviour for within-fire patch size distributions suggests that a similar balance may occur within fire events. For

small- to moderate-sized fires (e.g. 400–10,000 ha), patch size distributions varied widely, with some fires characterized primarily by large patches and others primarily by small patches; this suggests that in smaller fires, either broad- or local-scale factors alone may primarily drive spatial patterns of burn severity. Conversely, the convergence of patch size distributions toward a power law function with increasing fire size suggests that both broad- and local-scale factors influence spatial patterns of burn severity within large fires (e.g. >10,000 ha). Large fires often coincide with (Abatzoglou et al., 2021; Clarke et al., 2020) or can create their own (Fromm et al., 2010) extreme weather conditions, driving extreme fire behaviour. The largest burn days and largest high-severity patches therefore occur when broadscale drivers dominate (Peters et al., 2004). However, large fires can also burn over the course of many days to weeks (Scaduto et al., 2020), spanning a range of weather conditions and, by nature of covering large areas, encounter a range of topographic and vegetation structures. This wide range of conditions, alternating between places and times when broad- versus local-scale factors dominate, allows for the formation of a wide range of patch sizes, including many that are small but also some that are very large.

Despite occurring at the lowest frequency, the largest high-severity patches have the greatest ecological effect, both in terms of total high-severity burned area as well as distances to seed sources within patch interiors (Cansler & McKenzie, 2014; Collins et al., 2017; Harvey et al., 2016a). Although patch size distributions within large fires consistently converged towards a probability distribution taking the form of a power law, the size of the largest high-severity patches still varied among fires. The lack of convergence in the distance-to-seed parameter (SDC) with increasing fire size suggests that even in the largest fires, ecological effects can vary widely, due to both the size and spatial configuration (i.e. shape and surrounding forest cover) of the largest patches.

Stationary scaling relationships offer a means of projecting future fire effects

Across a wide range of fire regimes and forest ecosystems, we found that the relationships between fire size and high-severity patch size and structure appear stationary in both space and time, even over a time period (1985–2020) where climate and fire size distributions themselves were temporally variable (Juang et al., 2022). Put plainly, even as fire size distributions have shifted toward larger fires, the ranges of burn severity patterns expected for fires of a given size have remained the same. As climate and fire activity continue to shift, and as fuel limitations potentially increase in areas subject to increasing fire activity (Kennedy et al., 2021; Turner et al., 2022), it is possible that the envelopes of potential burn severity patterns may shift in the future. Continued

implementation of the methods presented here would permit such changes to be detected (e.g. downward shifts in scaling relationships might suggest an increasing prevalence of local-scale fuel constraints, thereby signalling potentially important changes in fire regimes). Within the contemporary fire record, however, our findings suggest that systematic shifts in scaling relationships have not yet occurred.

Managing for future fire requires not only projecting possible changes in regional metrics such as annual area burned, but also anticipating the potential ecological outcomes of those changes. Near-term shifts in fire size distributions alone (i.e. increasing frequency of large fires) will lead to predictable shifts in ecological effects (i.e. larger high-severity patches with interior burned areas far from potential seed sources). At broad scales, stationarity in scaling relationships offers a means of projecting the potential range of ecological effects expected with fire activity in the near future. Predicting burn severity patterns for a given landscape is difficult, since fire behaviour is highly stochastic and weather conditions at the time of burning can strongly influence the burn severity patterns that result (Parks, Holsinger, Panunto, et al., 2018; Prichard et al., 2020). However, by combining the range of variation in scaling relationships with projections for area burned and fire size distributions, it is possible to quantify the range of potential ecological effects of fire activity at a broader scale. Given the large range of variation in both climate and fire activity observed during the contemporary record, these scaling relationships integrate a wide range of potential burn-severity drivers. Our approach therefore provides a meaningful advance in inferential power by distilling fire size-severity relationships into relatively simple terms. Accounting for expected patterns of high-severity patch size and structure with increasing fire size enables bounds to be placed around potential outcomes, improving the ability to prepare for future fire activity.

CONCLUSION

Larger and simpler shaped high-severity burn patches can consistently be expected with larger fires, carrying important implications for forest resilience, ecosystem services and societies living sustainably with fire. Wildfire-driven transitions of forests to alternative vegetation states are increasingly likely within large and homogenous high-severity burn patches, where postfire tree regeneration is often limited by the availability of live seed sources. Spatial patterns of burn severity are therefore important to anticipate, as they can substantially alter habitat, hydrologic cycling, carbon storage and the societal benefits provided by forests (Coop et al., 2020). Within contemporary fire regimes, the stationarity we observed in burn severity scaling relationships offers a means to anticipate the range of burn severity patterns

expected with near-future fire activity. As fire activity continues to increase in many forested regions, and as the relative strength of climate drivers and fuel constraints potentially shift, these scaling relationships also offer a contemporary baseline that can be used to detect important changes that may occur within fire regimes in the future.

AUTHOR CONTRIBUTIONS

MSB and BJH conceived and designed the study, with input from all authors. MSB led data analysis with input from all authors. MSB wrote the first draft of the manuscript, and all authors contributed critically to drafts and approved the final manuscript.

ACKNOWLEDGEMENTS

This research was funded by a US Geological Survey Northwest Climate Adaptation Science Center award G17AC000218 to Michele S. Buonanduci and a Graduate Research Innovation award (#21-1-01-26) from the Joint Fire Science Program. Brian J. Harvey acknowledges support from the Jack Corkery and George Corkery Jr. Endowed Professorship in Forest Sciences. M.G. Turner and W.D. Hansen provided helpful reviews on an earlier draft of the manuscript.

PEER REVIEW

The peer review history for this article is available at <https://www.webofscience.com/api/gateway/wos/peer-review/10.1111/ele.14282>.

DATA AVAILABILITY STATEMENT

Data and code are available on Zenodo: <https://doi.org/10.5281/zenodo.7988103>

ORCID

Michele S. Buonanduci  <https://orcid.org/0000-0003-3646-9954>

Daniel C. Donato  <https://orcid.org/0000-0002-2072-9240>

Joshua S. Halofsky  <https://orcid.org/0000-0003-4120-7457>

Maureen C. Kennedy  <https://orcid.org/0000-0003-4670-3302>

Brian J. Harvey  <https://orcid.org/0000-0002-5902-4862>

REFERENCES

- Abatzoglou, J.T., Rupp, D.E., O'Neill, L.W. & Sadegh, M. (2021) Compound extremes drive the Western Oregon wildfires of September 2020. *Geophysical Research Letters*, 48, e2021GL092520.
- Abatzoglou, J.T., Williams, A.P., Boschetti, L., Zubkova, M. & Kolden, C.A. (2018) Global patterns of interannual climate–fire relationships. *Global Change Biology*, 24, 5164–5175.
- Arienti, M.C., Cumming, S.G. & Boutin, S. (2006) Empirical models of forest fire initial attack success probabilities: the effects of fuels, anthropogenic linear features, fire weather, and management. *Canadian Journal of Forest Research*, 36, 3155–3166.
- Boulanger, Y., Parisien, M.-A. & Wang, X. (2018) Model-specification uncertainty in future area burned by wildfires in Canada. *International Journal of Wildland Fire*, 27, 164–175.
- Bowman, D.M.J.S., Kolden, C.A., Abatzoglou, J.T., Johnston, F.H., van der Werf, G.R. & Flannigan, M. (2020) Vegetation fires in the Anthropocene. *Nature Reviews Earth & Environment*, 1, 500–515.
- Cade, B.S. & Noon, B.R. (2003) A gentle introduction to quantile regression for ecologists. *Frontiers in Ecology and the Environment*, 1, 412–420.
- Cansler, C.A. & McKenzie, D. (2012) How robust are burn severity indices when applied in a new region? Evaluation of alternate field-based and remote-sensing methods. *Remote Sensing*, 4, 456–483.
- Cansler, C.A. & McKenzie, D. (2014) Climate, fire size, and biophysical setting control fire severity and spatial pattern in the northern Cascade Range, USA. *Ecological Applications*, 24, 1037–1056.
- Clarke, H., Penman, T., Boer, M., Cary, G.J., Fontaine, J.B., Price, O. et al. (2020) The proximal drivers of large fires: a Pyrogeographic study. *Frontiers in Earth Science*, 8, 90.
- Collins, B.M., Stevens, J.T., Miller, J.D., Stephens, S.L., Brown, P.M. & North, M.P. (2017) Alternative characterization of forest fire regimes: incorporating spatial patterns. *Landscape Ecology*, 32, 1543–1552.
- Collins, L., Bradstock, R.A., Clarke, H., Clarke, M.F., Nolan, R.H. & Penman, T.D. (2021) The 2019/2020 mega-fires exposed Australian ecosystems to an unprecedented extent of high-severity fire. *Environmental Research Letters*, 16, 044029.
- Commission for Environmental Cooperation. (1997) *Ecological regions of North America: toward a common perspective*.
- Coop, J.D., Parks, S.A., Stevens-Rumann, C.S., Crausbay, S.D., Higuera, P.E., Hurteau, M.D. et al. (2020) Wildfire-driven Forest conversion in Western North American landscapes. *Bioscience*, 70, 659–673.
- Davis, K.T., Robles, M.D., Kemp, K.B., Higuera, P.E., Chapman, T., Metlen, K.L. et al. (2023) Reduced fire severity offers near-term buffer to climate-driven declines in conifer resilience across the western United States. *Proceedings. National Academy of Sciences. United States of America*, 120, e2208120120.
- Donato, D.C., Fontaine, J.B., Campbell, J.L., Robinson, W.D., Kauffman, J.B. & Law, B.E. (2009) Conifer regeneration in stand-replacement portions of a large mixed-severity wildfire in the Klamath–Siskiyou Mountains. *Canadian Journal of Forest Research*, 39, 823–838.
- Fromm, M., Lindsey, D.T., Servranckx, R., Yue, G., Trickl, T., Sica, R. et al. (2010) The untold story of Pyrocumulonimbus. *Bulletin of the American Meteorological Society*, 91, 1193–1210.
- Gardner, R.H. & Urban, D.L. (2007) Neutral models for testing landscape hypotheses. *Landscape Ecology*, 22, 15–29.
- Gill, N.S., Turner, M.G., Brown, C.D., Glassman, S.I., Haire, S.L., Hansen, W.D. et al. (2022) Limitations to propagule dispersal will constrain postfire recovery of plants and fungi in Western coniferous forests. *Bioscience*, 72, 347–364.
- Hagmann, R.K., Hessburg, P.F., Prichard, S.J., Povak, N.A., Brown, P.M., Fulé, P.Z. et al. (2021) Evidence for widespread changes in the structure, composition, and fire regimes of western North American forests. *Ecological Applications*, 31, e02431.
- Hanson, S., Pueyo, S. & Chuvieco, E. (2016) Global fire size distribution: from power law to log-normal. *International Journal of Wildland Fire*, 25, 403.
- Harvey, B.J., Buonanduci, M.S. & Turner, M.G. (2023) Spatial interactions among short-interval fires reshape forest landscapes. *Global Ecology and Biogeography*, 32, 586–602.
- Harvey, B.J., Donato, D.C. & Turner, M.G. (2016a) Drivers and trends in landscape patterns of stand-replacing fire in forests of the US northern Rocky Mountains (1984–2010). *Landscape Ecology*, 31, 2367–2383.

- Harvey, B.J., Donato, D.C. & Turner, M.G. (2016b) High and dry: post-fire tree seedling establishment in subalpine forests decreases with post-fire drought and large stand-replacing burn patches: drought and post-fire tree seedlings. *Global Ecology and Biogeography*, 25, 655–669.
- Hijmans, R.J., van Etten, J., Sumner, M., Cheng, J., Baston, D., Bevan, A. et al. (2022) Package “raster.”
- Hood, S.M., Harvey, B.J., Fornwalt, P.J., Naficy, C.E., Hansen, W.D., Davis, K.T. et al. (2021) Fire ecology of Rocky Mountain forests. In: Greenberg, C.H. & Collins, B. (Eds.) *Fire ecology and management: past, present, and future of US forested ecosystems, managing Forest ecosystems*. Cham: Springer International Publishing, pp. 287–336.
- Johnstone, J.F., Allen, C.D., Franklin, J.F., Frelich, L.E., Harvey, B.J., Higuera, P.E. et al. (2016) Changing disturbance regimes, ecological memory, and forest resilience. *Frontiers in Ecology and the Environment*, 14, 369–378.
- Juang, C.S., Williams, A.P., Abatzoglou, J.T., Balch, J.K., Hurteau, M.D. & Moritz, M.A. (2022) Rapid growth of large Forest fires drives the exponential response of annual Forest-fire area to aridity in the Western United States. *Geophysical Research Letters*, 49, e2021GL097131.
- Kennedy, M.C., Bart, R.R., Tague, C.L. & Choate, J.S. (2021) Does hot and dry equal more wildfire? Contrasting short- and long-term climate effects on fire in the Sierra Nevada, CA. *Ecosphere*, 12, e03657.
- Koenker, R. & Bassett, G. (1978) Regression quantiles. *Econometrica*, 46, 33.
- Lecina-Díaz, J., Martínez-Vilalta, J., Alvarez, A., Banqué, M., Birkmann, J., Feldmeyer, D. et al. (2021) Characterizing forest vulnerability and risk to climate-change hazards. *Frontiers in Ecology and the Environment*, 19, 126–133.
- Littell, J.S., McKenzie, D., Wan, H.Y. & Cushman, S.A. (2018) Climate change and future wildfire in the Western United States: an ecological approach to nonstationarity. *Earth's Future*, 6, 1097–1111.
- Lydersen, J.M., Collins, B.M., Miller, J.D., Fry, D.L. & Stephens, S.L. (2016) Relating fire-caused change in Forest structure to remotely sensed estimates of fire severity. *Fire Ecology*, 12, 99–116.
- McKenzie, D. & Kennedy, M.C. (2011) Scaling laws and complexity in fire regimes. In: McKenzie, D., Miller, C. & Falk, D.A. (Eds.) *The landscape ecology of fire, ecological studies*. Netherlands, Dordrecht: Springer, pp. 27–49.
- McKenzie, D. & Kennedy, M.C. (2012) Power laws reveal phase transitions in landscape controls of fire regimes. *Nature Communications*, 3, 726.
- Miller, J.D., Safford, H.D., Crimmins, M. & Thode, A.E. (2009) Quantitative evidence for increasing Forest fire severity in the Sierra Nevada and southern Cascade Mountains, California and Nevada, USA. *Ecosystems*, 12, 16–32.
- Miller, J.D., Skinner, C.N., Safford, H.D., Knapp, E.E. & Ramirez, C.M. (2012) Trends and causes of severity, size, and number of fires in northwestern California, USA. *Ecological Applications*, 22, 184–203.
- Miller, J.D. & Thode, A.E. (2007) Quantifying burn severity in a heterogeneous landscape with a relative version of the delta normalized burn ratio (dNBR). *Remote Sensing of Environment*, 109, 66–80.
- Moritz, M.A., Hessburg, P.F. & Povak, N.A. (2011) Native fire regimes and landscape resilience. In: McKenzie, D., Miller, C. & Falk, D.A. (Eds.) *The landscape ecology of fire, ecological studies*. Netherlands, Dordrecht: Springer, pp. 51–86.
- Muggeo, V.M.R. (2021) Additive quantile regression with automatic smoothness selection: the R package quantregGrowth.
- Muggeo, V.M.R., Torretta, F., Eilers, P.H.C., Sciandra, M. & Attanasio, M. (2021) Multiple smoothing parameters selection in additive regression quantiles. *Statistical Modelling*, 21, 428–448.
- Newman, E.A., Kennedy, M.C., Falk, D.A. & McKenzie, D. (2019) Scaling and complexity in landscape ecology. *Frontiers in Ecology and Evolution*, 7, 293.
- Parks, S., Holsinger, L., Voss, M., Loehman, R. & Robinson, N. (2018) Mean composite fire severity metrics computed with Google earth engine offer improved accuracy and expanded mapping potential. *Remote Sensing*, 10, 879.
- Parks, S.A. & Abatzoglou, J.T. (2020) Warmer and drier fire seasons contribute to increases in area burned at high severity in Western US forests from 1985 to 2017. *Geophysical Research Letters*, 47, e2020GL089858.
- Parks, S.A., Holsinger, L.M., Panunto, M.H., Jolly, W.M., Dobrowski, S.Z. & Dillon, G.K. (2018) High-severity fire: evaluating its key drivers and mapping its probability across western US forests. *Environmental Research Letters*, 13, 044037.
- Pausas, J.G., Keeley, J.E. & Schwilk, D.W. (2017) Flammability as an ecological and evolutionary driver. *Journal of Ecology*, 105, 289–297.
- Pebesma, E. (2018) Simple features for R: standardized support for spatial vector data. *The R Journal*, 10, 439.
- Peters, D.P.C., Pielke, R.A., Bestelmeyer, B.T., Allen, C.D., Munson-McGee, S. & Havstad, K.M. (2004) Cross-scale interactions, nonlinearities, and forecasting catastrophic events. *Proceedings. National Academy of Sciences. United States of America*, 101, 15130–15135.
- Povak, N.A., Hessburg, P.F. & Salter, R.B. (2018) Evidence for scale-dependent topographic controls on wildfire spread. *Ecosphere*, 9, e02443.
- Prichard, S.J., Povak, N.A., Kennedy, M.C. & Peterson, D.W. (2020) Fuel treatment effectiveness in the context of landform, vegetation, and large, wind-driven wildfires. *Ecological Applications*, 30, e02104.
- Pueyo, S. (2006) Diversity: between neutrality and structure. *Oikos*, 112, 392–405.
- Pueyo, S. (2014) Algorithm for the maximum likelihood estimation of the parameters of the truncated normal and lognormal distributions.
- Reilly, M.J., Dunn, C.J., Meigs, G.W., Spies, T.A., Kennedy, R.E., Bailey, J.D. et al. (2017) Contemporary patterns of fire extent and severity in forests of the Pacific Northwest, USA (1985–2010). *Ecosphere*, 8, e01695.
- Reilly, M.J., Halofsky, J.E., Krawchuk, M.A., Donato, D.C., Hessburg, P.F., Johnston, J.D. et al. (2021) Fire ecology and Management in Pacific Northwest Forests. In: Greenberg, C.H. & Collins, B. (Eds.) *Fire ecology and management: past, present, and future of US forested ecosystems, managing Forest ecosystems*. Cham: Springer International Publishing, pp. 393–435.
- Rivera-Huerta, H., Safford, H.D. & Miller, J.D. (2016) Patterns and trends in burned area and fire severity from 1984 to 2010 in the sierra de San Pedro Mártir, Baja California, Mexico. *Fire Ecology*, 12, 52–72.
- Rollins, M.G. (2009) LANDFIRE: a nationally consistent vegetation, wildland fire, and fuel assessment. *International Journal of Wildland Fire*, 18, 235.
- Rose, N.L., Yang, H., Turner, S.D. & Simpson, G.L. (2012) An assessment of the mechanisms for the transfer of lead and mercury from atmospherically contaminated organic soils to lake sediments with particular reference to Scotland, UK. *Geochimica et Cosmochimica Acta*, 82, 113–135.
- Saberi, S.J. & Harvey, B.J. (2023) What is the color when black is burned? Quantifying (re)burn severity using field and satellite remote sensing indices. *Fire Ecology*, 19, 24.
- Scaduto, E., Chen, B. & Jin, Y. (2020) Satellite-based fire progression mapping: a comprehensive assessment for large fires in northern California. *IEEE Journal of Selected Topics in Applied Earth Observations Remote Sensing*, 13, 5102–5114.
- Singleton, M.P., Thode, A.E., Sánchez Meador, A.J. & Iniguez, J.M. (2019) Increasing trends in high-severity fire in the southwestern

- USA from 1984 to 2015. *Forest Ecology and Management*, 433, 709–719.
- Steel, Z.L., Fogg, A.M., Burnett, R., Roberts, L.J. & Safford, H.D. (2022) When bigger isn't better—implications of large high-severity wildfire patches for avian diversity and community composition. *Diversity and Distributions*, 28, 439–453.
- Stevens, J.T., Collins, B.M., Miller, J.D., North, M.P. & Stephens, S.L. (2017) Changing spatial patterns of stand-replacing fire in California conifer forests. *Forest Ecology and Management*, 406, 28–36.
- Stevens, J.T., Kling, M.M., Schwilk, D.W., Varner, J.M. & Kane, J.M. (2020) Biogeography of fire regimes in western U.S. conifer forests: a trait-based approach. *Global Ecology and Biogeography*, 29, 944–955.
- Turner, M.G., Braziunas, K.H., Hansen, W.D., Hoecker, T.J., Rammer, W., Ratajczak, Z. et al. (2022) The magnitude, direction, and tempo of forest change in greater Yellowstone in a warmer world with more fire. *Ecological Monographs*, 92, e01485.
- Turner, M.G., Tinker, D.B., Romme, W.H., Kashian, D.M. & Litton, C.M. (2004) Landscape patterns of sapling density, leaf area, and aboveground net primary production in postfire lodgepole pine forests, Yellowstone National Park (USA). *Ecosystems*, 7, 751–775.
- Wang, X., Swystun, T. & Flannigan, M.D. (2022) Future wildfire extent and frequency determined by the longest fire-conducive weather spell. *Science of the Total Environment*, 830, 154752.
- Whitman, E., Parks, S.A., Holsinger, L.M. & Parisien, M.-A. (2022) Climate-induced fire regime amplification in Alberta, Canada. *Environmental Research Letters*, 17, 55003.

SUPPORTING INFORMATION

Additional supporting information can be found online in the Supporting Information section at the end of this article.

How to cite this article: Buonanduci, M.S., Donato, D.C., Halofsky, J.S., Kennedy, M.C. & Harvey, B.J. (2023) Consistent spatial scaling of high-severity wildfire can inform expected future patterns of burn severity. *Ecology Letters*, 00, 1–13. Available from: <https://doi.org/10.1111/ele.14282>